Localization, Ion Channel Regulation, and Genetic Interactions during Abscisic Acid Signaling of the Nuclear mRNA Cap-Binding Protein, ABH1[1]

Véronique Hugouvieux, Yoshiyuki Murata[2], Jared J. Young, June M. Kwak, Daniel Z. Mackesy, and Julian I. Schroeder*

Division of Biology, Cell, and Developmental Biology Section, and Center for Molecular Genetics, University of California San Diego, 9500 Gilman Drive, La Jolla, California 92093–0116

Abscisic acid (ABA) regulates developmental processes and abiotic stress responses in plants. We recently characterized a new Arabidopsis mutant, *abh1*, which shows ABA-hypersensitive regulation of seed germination, stomatal closing, and cytosolic calcium increases in guard cells (V. Hugouvieux, J.M. Kwak, J.I. Schroeder [2001] Cell 106: 477–487). *ABH1* encodes the large subunit of a dimeric Arabidopsis mRNA cap-binding complex and in expression profiling experiments was shown to affect mRNA levels of a subset of genes. Here, we show that the dimeric ABH1 and AtCBP20 subunits are ubiquitously expressed. Whole-plant growth phenotypes of *abh1* are described and properties of ABH1 in guard cells are further analyzed. Complemented *abh1* lines expressing a green fluorescent protein-ABH1 fusion protein demonstrate that ABH1 mainly localizes in guard cell nuclei. Stomatal apertures were smaller in *abh1* compared with wild type (WT) when plants were grown at 40% humidity, and similar at 95% humidity. Correlated with stomatal apertures from plants grown at 40% humidity, slow anion channel currents were enhanced and inward potassium channel currents were decreased in *abh1* guard cells compared with WT. Gas exchange measurements showed similar primary humidity responses in *abh1* and WT, which together with results from *abh1/abi1-1* double-mutant analyses suggest that *abh1* shows enhanced sensitivity to endogenous ABA. Double-mutant analyses of the ABA-hypersensitive signaling mutants, *era1-2* and *abh1*, showed complex genetic interactions, suggesting that ABH1 and ERA1 do not modulate the same negative regulator in ABA signaling. Mutations in the RNA-binding protein *sad1* showed hypersensitive ABA-induced stomatal closing, whereas *hyl1* did not affect this response. These data provide evidence for the model that the mRNA-processing proteins ABH1 and SAD1 function as negative regulators in guard cell ABA signaling.

The plant hormone abscisic acid (ABA) controls several physiologically important stress and developmental responses throughout the life cycle of plants. During seed development, ABA triggers the acquisition of nutritive reserves, desiccation tolerance, maturation, and dormancy (Marcotte et al., 1992; Koornneef et al., 1998; Finkelstein et al., 2002). Later, during vegetative growth, ABA is the internal signal that enables plant adaptive responses to adverse environmental conditions such as drought, salt, and cold stresses (Marcotte et al., 1992; Koornneef et al., 1998; Leung and Giraudat, 1998).

In response to drought, ABA is synthesized and induces closure of stomatal pores, located on the leaf surface, to limit water loss by transpiration. Stomatal pores are surrounded by pairs of guard cells whose turgor regulates stomatal pore apertures. ABA induces stomatal closure via efflux of K^+ and anions from guard cells and removal of organic osmolytes (MacRobbie, 1998; Schroeder et al., 2001). Ion channel-mediated efflux of anions and K^+ and stomatal closure are controlled by ABA-induced cytosolic calcium ($[Ca^{2+}]_{cyt}$) increases (Schroeder and Hagiwara, 1989; McAinsh et al., 1990; MacRobbie, 1998).

An increasing number of genetic mutations that contribute to ABA signaling in guard cells have been characterized recently. These genes include two type 2C protein phosphatases, *abi1-1* and *abi2-1* (Leung et al., 1994, 1997; Meyer et al., 1994), a farnesyl transferase β-subunit, *ERA1* (Cutler et al., 1996; Pei et al., 1998), an ABA-activated protein kinase mutant (*aapk*; Li et al., 2000), a GTP-binding protein α-subunit, *GPA1* (Wang et al., 2001), dominant mutations in a GTPase protein, *Atrac1-1* (Lemichez et al., 2001), and an mRNA cap-binding protein, *ABH1* (Hugouvieux et al., 2001). Genes that affect ABA responses at the transcriptional level in seed germination and development have also been identified encoding three transcriptional regulators, *ABI3* (Giraudat et al., 1992), *ABI4* (Finkelstein et al., 1998), and *ABI5* (Finkelstein and Lynch, 2000). Two RNA-binding

[1] This research was supported by the National Institutes of Health (grant no. R01GM60396–01), by the Torrey Mesa Research Institute/University of California Biostar (grant), in part by the National Science Foundation (grant no. MCB 0077791 to J.I.S.), and by the Human Frontier Science Program Organization (fellowship to J.M.K.).

[2] Present address: Department of Agriculture, Okayama University, Tsushima-Naka, Okayama 700–8530, Japan.

* Corresponding author; e-mail julian@biomail.ucsd.edu; fax 858–534–7108.

Article, publication date, and citation information can be found at www.plantphysiol.org/cgi/doi/10.1104/pp.009480.

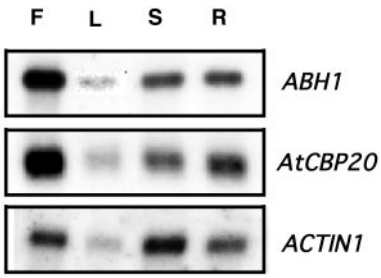

Figure 1. Expression level of the CBC subunits, *ABH1* and *AtCBP20*, is ubiquitous. Northern-blot analyses were performed on approximately 2 μg of poly(A^+) RNA (extracted from flowers [F], stems [S], leaves [L], and roots [R]) in WT Arabidopsis. ABH1 or *AtCBP20* cDNAs were used as probes. *Actin1* probe was used as a loading control.

proteins, a double-stranded RNA-binding protein, HYL1 (Lu and Fedoroff, 2000), and a protein similar to an Sm-like snRNP protein, SAD1 (Xiong et al., 2001a) were recently described to affect ABA regulation of seed germination. The *sad1* mutation also caused enhanced ABA-induced expression of marker genes, but is drought hypersensitive (Xiong et al., 2001a). The *fry1* mutant shows a superinduction of ABA- and stress-responsive genes and revealed the involvement of an inositol polyphosphate 1-phosphatase in ABA signaling (Xiong et al., 2001b).

We recently characterized the *abh1* mutation (Hugouvieux et al., 2001) that points to a link between mRNA metabolism and ABA signaling. *ABH1* encodes a homolog to yeast (*Saccharomyces cerevisiae*) and human (*Homo sapiens*) *CBP80* genes and functions as the large subunit of an Arabidopsis mRNA cap-binding complex (CBC). No other *ABH1* homologs are present in the Arabidopsis genome. Disruption of *ABH1* results in ABA-hypersensitive regulation of seed germination, ABA-hypersensitive stomatal closing, reduced wilting during drought, and, interestingly, ABA-hypersensitive $[Ca^{2+}]_{cyt}$ increases in guard cells, demonstrating amplification of early ABA signaling mechanisms (Hugouvieux et al., 2001). In yeast and mammals, CBC is involved in mRNA metabolism (Lewis and Izaurralde, 1997). DNA microarray experiments comparing the level of expression of genes in wild type (WT) and *abh1* showed that a limited number of genes in *abh1* are down-regulated, some of which may correspond to negative regulators of ABA signaling in guard cells. The recent isolation of three recessive ABA-hypersensitive mutants, *abh1*, *hyl1*, and *sad1*, which all encode RNA-associated proteins, gives rise to a new model by which RNA processing modulates and/or participates in ABA signal transduction.

To better understand ABH1 functions in plants, in the present work we characterize the pattern of *ABH1* gene expression and associated whole-plant growth phenotypes of *abh1*. We also analyze ABH1 protein localization in guard cells and genetic interactions between ABH1 and the early ABA signaling components *abi1-1* and ERA1 during stomatal regulation. In addition, we further characterize stomatal responses of *abh1*, *sad1*, and *hyl1* which show differential effects on ABA-induced stomatal closing in *hyl1* compared with *abh1* and *sad1*. Responses in *sad1* strengthen the hypothesis that RNA processing contributes to ABA signal transduction in guard cells.

RESULTS

ABH1 Expression Is Ubiquitous

ABH1 was shown to be expressed in guard cells (Hugouvieux et al., 2001). Northern-blot analyses were performed on poly(A^+) RNA extracted from WT roots, leaves, flowers, and stems to analyze *ABH1* gene expression in various organs. As shown in Figure 1, *ABH1* transcript was present in all tissues analyzed, with high expression in flowers. The At*CBP20* gene encodes the small subunit of the CBC and is required for in vitro binding of ABH1 to the 7-methyl guanosine cap structure of mRNA (Hugouvieux et al., 2001). *AtCBP20* showed the same expression pattern as *ABH1* (Fig. 1).

WT transgenic seedlings expressing the β-glucuronidase (GUS) reporter gene under the control of the *ABH1* promoter (genomic sequence containing 1.2 kb from the 5′ end of the *ABH1* start site; Hugouvieux et al., 2001) were used to further analyze in which tissues the *ABH1* promoter was active. As expected, GUS activity was detected in roots and hypocotyls (Fig. 2A), cotyledons (Fig. 2B), and leaves (Fig. 2C).

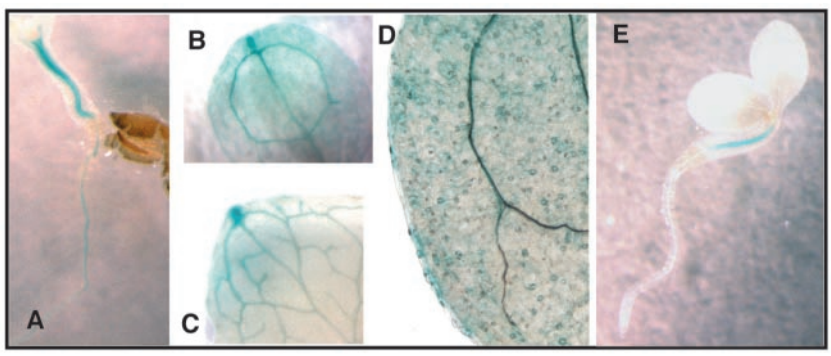

Figure 2. Analysis of GUS activity in WT plants transformed with the GUS reporter gene under the control of the *ABH1* promoter. A through E, GUS activity in the hypocotyl and root of an 8-d old seedling (A), a cotyledon of an 8-d old seedling (B), a mature leaf (C), guard cells (D), and the hypocotyl of 2-d-old seedling (E).

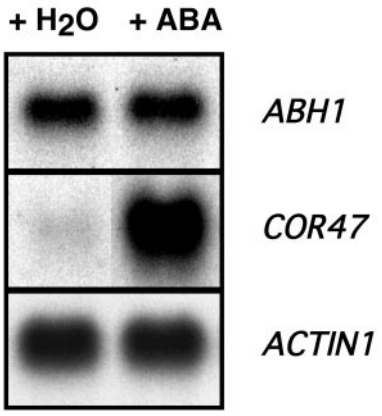

Figure 3. ABH1 expression level is not regulated by ABA. WT leaves from five individual plants were sprayed with 100 μM ABA or water in parallel control experiments. Four hours later, poly(A^+) RNA was extracted and 2 μg was used in northern-blot analyses using *ABH1* cDNA and the *COR47* genomic fragment as a probe. *Actin1* probe was used as a loading control. Similar results were obtained in two replicates, and in the WT ecotype Wassilewskija (data not shown).

GUS activity was not detected in root or apical meristems (data not shown). The *ABH1* promoter was highly active in vascular tissues (hypocotyls, roots, cotyledons, and leaves; Fig. 2, A–C). *ABH1* expression was also observed in the vascular tissues of petals (data not shown). In 2-d-old seedlings, GUS activity was often first visually detectable in the hypocotyl (Fig. 2E); however, this restricted expression pattern disappeared in 8-d-old seedlings, suggesting a developmental control of *ABH1* expression. The *ABH1* promoter was active in guard cells (Fig. 2D; Hugouvieux et al., 2001). The same patterns of expression were observed in three independent homozygous lines.

ABA Treatment Does Not Change *ABH1* Transcript Level

ABH1 is a negative regulator of ABA signaling (Hugouvieux et al., 2001). We further investigated whether ABA treatment induces changes in the *ABH1* transcript level. As shown in Figure 3, treatment of WT leaves with 100 μM ABA for 4 h did not change *ABH1* transcript levels (Fig. 3; $n = 2$ experiments). In control experiments, the transcript level of ABA-inducible genes was increased in WT plants, including *COR47* (Fig. 3), *RAB18*, *ABI1*, and *ABI2* (data not shown). Treatments with lower concentrations of ABA (0.1, 1, and 10 μM) were also performed and again showed no ABA regulation of *ABH1* at the transcript level. The lack of ABA regulation of *ABH1* mRNA levels was also observed after drought treatment (data not shown). As positive controls, under drought conditions, induction of the drought-induced gene, *COR47*, was observed (data not shown).

Growth and Developmental Phenotypes of *abh1*

Considering the expression pattern of the *ABH1* gene in vegetative tissues (Figs. 1 and 2), several morphological and growth characteristics of *abh1* and WT plants were analyzed. *abh1* plants showed a slightly serrated leaf phenotype (Fig. 4, top left) that is complemented in *abh1* plants expressing the WT copy of the *ABH1* gene (Fig. 4, lower right). Interestingly, this leaf phenotype was also observed in homozygous *abh1/era1-2* and *abh1/abi1-1* double mutants, which were indistinguishable from the *abh1* mutant in leaf morphology (data not shown).

After exposure of seeds to 4°C for 4 d, 6-month-old *abh1* and WT seeds germinated at the same rate in the absence of exogenous ABA (Hugouvieux et al., 2001). Under these conditions, *abh1* plants were smaller than WT after 3 weeks of growth (Fig. 5A) and showed a delay in bolting and flowering time after 6 weeks (Fig. 5B). However, *abh1* and WT appeared very similar at maturity (Fig. 5C). An approximately 5- to 10-d delay was observed in flowering of *abh1* plants compared with WT. This delay varied among plants showing slightly different genetic penetrance among individual plants. The same number of leaves

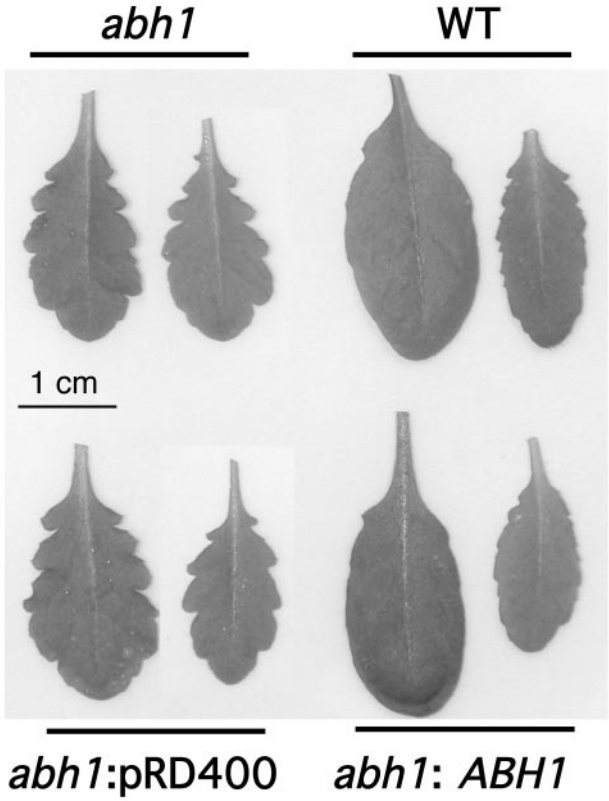

Figure 4. abh1 plants show a serrated leaf phenotype that is complemented by the *ABH1* gene. Two rosette leaves of each plant are shown after 7 weeks of growth. *abh1* lines complemented with the *ABH1* promoter and gene (*abh1*:*ABH1*) were generated as described (Hugouvieux et al., 2001). *abh1* lines transformed with the vector control pRD400 only (*abh1*:pDR400) were used as controls.

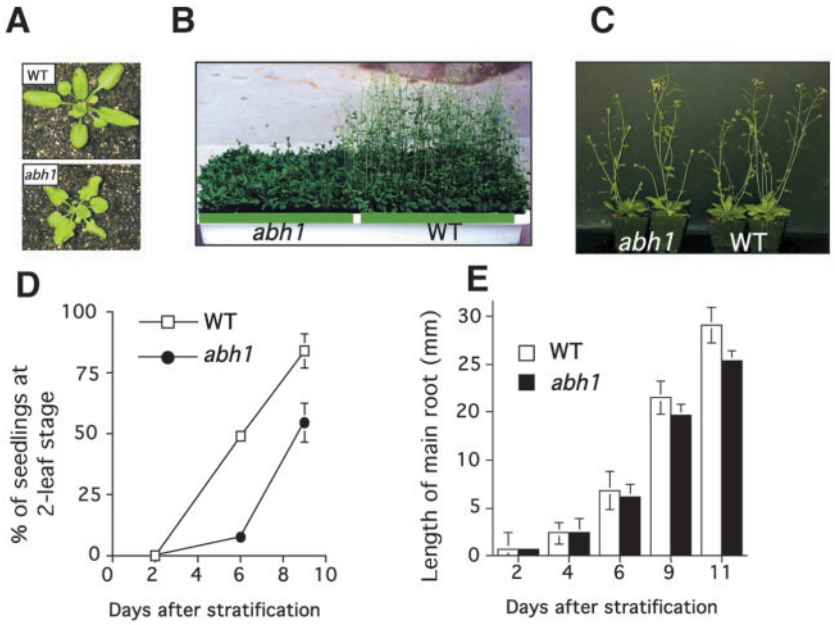

Figure 5. abh1 growth is slower compared with WT. A, *abh1* and WT rosettes are shown after 3 weeks of growth. For the same age, *abh1* rosettes are smaller and show a smaller number of leaves. B, WT and *abh1* plants are shown after 6 weeks of growth. The delay in flowering is about 5 to 10 d in *abh1*. C, When *abh1* and WT growth was synchronized, WT and *abh1* plants showed similar whole-plant phenotypes (see also Table I). D, Development of the first two leaves in *abh1* and WT seedlings grown in petri dishes. Data represent the mean of five experiments ± SE (n = 30 seedlings per line for each experiment). E, Root elongation after 2, 6, 9, and 11 d in *abh1* and WT. The figure shows a representative experiment ± SD (n = 60). D and E, Error bars are smaller than symbols when not visible. The slower growth in *abh1* was complemented by the *ABH1* gene (data not shown). A, B, D, and E, WT and *abh1* plants were grown in parallel in a growth chamber after stratification for 4 d at 4°C from seeds between 3 to 6 months old.

(between eight and 10) was observed in *abh1* and WT plants when they started bolting, suggesting that *abh1* growth is slowed compared with WT and that *abh1* is not a late-flowering mutant that shows an increased leaf number when flowering. To further investigate whether *abh1* growth was slower compared with WT, we followed the shoot and the main root's development in *abh1* and WT seedlings grown in petri dishes. As shown in Figure 5D, the appearance and development of the first two leaves were delayed in *abh1* compared with WT after 6 and 9 d of growth. Root length was slightly decreased in *abh1* compared with WT after 11 d of growth, although root length was similar after 2 d in both WT and *abh1* (Fig. 5E). These data suggested that *abh1* growth is delayed compared with WT. Morphological characteristics of *abh1* and WT plants were further analyzed and compared at maturity. As summarized in Table I, the only significant difference observed between *abh1* and WT was in the length of the main stem, which was decreased in *abh1* by approximately 15% to 20%. No significant differences were observed in the number of seeds per plant, the number of petals per flower, or the number of secondary and lateral branches. These data showed that the *abh1* mutation does not significantly affect important developmental processes during growth and further reaffirms the relative dearth of pleiotropic effects of the *abh1* mutation.

ABH1 Is Mainly Localized in the Nucleus

We showed that ABH1, together with AtCBP20, binds the 7-methyl guanosine cap structure of mRNA in vitro, and that its disruption leads to abnormal transcript accumulation of a limited number of genes in planta (Hugouvieux et al., 2001), which suggests that ABH1 has a role in mRNA processing. To obtain

Table I. *Morphological characteristics of abh1 and WT*

More than 20 *abh1* and WT plants were grown in parallel in each experiment (Exp) after their growth was synchronized (see "Materials and Methods"). Plants used for measurements were selected randomly. Measurements were performed after 9 weeks, except for the petals, which were counted when flowers had opened (6–8 weeks). SEs of the mean are shown.

Property	WT	*abh1*
Length of the main stem (cm)[a]	Exp 1: 34.03 ± 1.18	29.5 ± 1.49[e]
	Exp 2: 26.65 ± 0.79	21.07 ± 0.7[e]
No. of lateral branches[a]	Exp 1: 2.6 ± 0.22	2.9 ± 0.18
	Exp 2: 1.8 ± 0.29	2 ± 0.39
No. of secondary stems[a]	Exp 1: 4.28 ± 0.42	4.14 ± 0.34
	Exp 2: 4.85 ± 0.4	4.42 ± 0.429
Length of the siliques[b]	1.45 ± 0.017	1.41 ± 0.01
No. of seeds/siliques[b]	40.75 ± 1.84	41.87 ± 2.16
Weight of seeds/plants (mg)[c]	68 ± 0.007	70 ± 0.006
No. of petals per flower[d]	4.009 ± 0.09	4.049 ± 0.21

[a] n = 7 and 10 in Exp 1 and 2, respectively. [b] n = 30. [c] n = 10. [d] n = 100. [e] Significant difference from WT.

further insights into ABH1 function in guard cells, we analyzed where the protein was localized.

To investigate the subcellular localization of the ABH1 protein, ABH1 and green fluorescent protein (GFP) coding sequences were fused in frame to produce both N- and C-terminal fusions. *abh1* mutant plants expressing the N-terminal fusion protein, GFP-ABH1, showed complementation of the abh1 mutant based on seed germination assays with ABA and on suppression of the serrated leaf phenotype (data not shown), illustrating that GFP-ABH1 was functional. The C-terminal fusion protein, ABH1-GFP, showed no complementation of the abh1 mutant based on ABA-dependent seed germination analyses and on the persistence of the serrated leaf phenotype (data not shown). These data suggest that the C-terminal domain of ABH1 is important for ABH1 function. Thus, further analyses were performed on the functional GFP-ABH1 lines. The subcellular localization of GFP-ABH1 was analyzed in guard cells and epidermal cells (Fig. 6, A–I). Untransformed WT plants, as expected, showed no GFP fluorescence (Fig. 6, A and E). The GFP-ABH1 fusion protein was mainly found in nuclei in both WT and *abh1* plants and a slight GFP activity was detected in the cytosol (Fig. 6, G–I). The same pattern of expression was observed using the C-terminal fusion (data not shown). In control experiments, in which WT plants expressed the GFP protein fused to the GUS protein, the GFP-GUS fusion protein was detected in the cytosol (Fig. 6F). The nuclear localization of GFP-ABH1 and complementation of abh1 by this fusion protein support the proposed function of ABH1 as a subunit of a nuclear RNA CBC.

Anion and Potassium Channel Activity in *abh1*

To better understand the function of ABH1 in guard cell signaling, we further investigated guard cell phenotypes in *abh1* plants. When stomatal apertures were measured in leaves harvested directly from plants grown under low humidity (40%), stomatal apertures of *abh1* were smaller than those of WT plants (Fig. 7A). WT stomatal apertures were restored in three homozygous *abh1* lines transformed with the *ABH1* gene (Fig. 7A). In contrast, for plants exposed to 95% humidity (overnight treatment), stomatal apertures in *abh1* and WT were similar (*abh1* stomatal aperture width/length, 0.17 ± 0.04; WT stomatal aperture width/length, 0.16 ± 0.02; $n = 3$ experiments ± SD). The smaller stomatal apertures observed in *abh1* plants exposed to 40% humidity possibly resulted either from hypersensitivity to endogenous ABA or because *abh1* showed an altered response to low humidity.

To distinguish between these two possibilities, we investigated the humidity response of *abh1* plants by comparing stomatal conductances of WT and *abh1* at various humidities using an infrared gas analyzer (Fig. 7B). Gas exchange in *abh1* plants at 40% humidity was slightly reduced compared with WT (Fig. 7B), consistent with stomatal aperture measurements (Fig. 7A). Stomata of *abh1* closed upon introduction of lower humidity, as did WT stomata (Fig. 7B). The rapid response in gas exchange experiments to step changes in humidity was previously shown to be independent of ABA signaling in Arabidopsis (Assmann et al., 2000). Indistinguishable gas exchange responses to step changes in humidity in *abh1* and WT (Fig. 7B) suggest that *abh1* does not directly modulate the rapid primary humidity response. We also observed that stomatal apertures of *abi1-1* were generally larger than those of WT plants (Landsberg *erecta* [L*er*] background) when no ABA was added, including plants grown at 40% humidity (described later), and *abi1-1* does not affect the stomatal response to humidity (Assmann et al., 2000). These findings are consistent with the hypothesis that re-

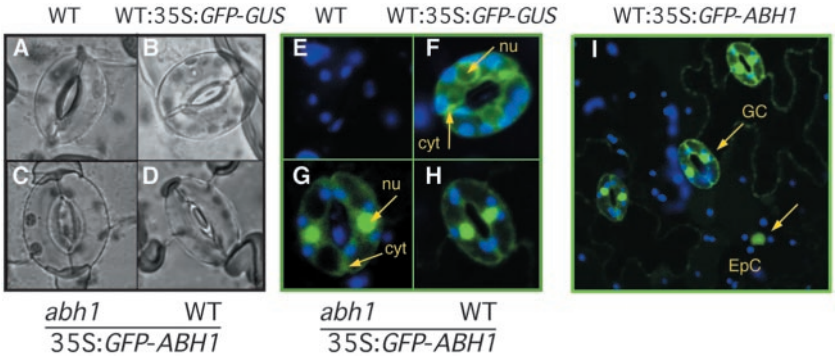

Figure 6. GFP-ABH1 fusion protein is localized mainly in nuclei in WT and *abh1*. A through D, Bright-field images of guard cells used to study GFP fluorescence in E through H. Blue and green colors show chloroplast (emission 488 nm) and GFP (emission 522 nm) fluorescence, respectively. F, WT control transformed with GFP fused to the GUS protein (pCAMBIA1303; GenBank accession no. AF23299) shows that GFP-GUS is not localized in nuclei (nu), but rather in the cytosol (cyt). G, *abh1*-complemented lines with 35S:*GFP-ABH1* construct show GFP fluorescence mainly in nuclei. H and I, Epidermal strips from WT transformed with the 35S:*GFP-ABH1* construct show GFP fluorescence mainly in the nuclei in guard cells (GC) and epidermal cells (EpC). The same pattern of expression was observed in three independent lines.

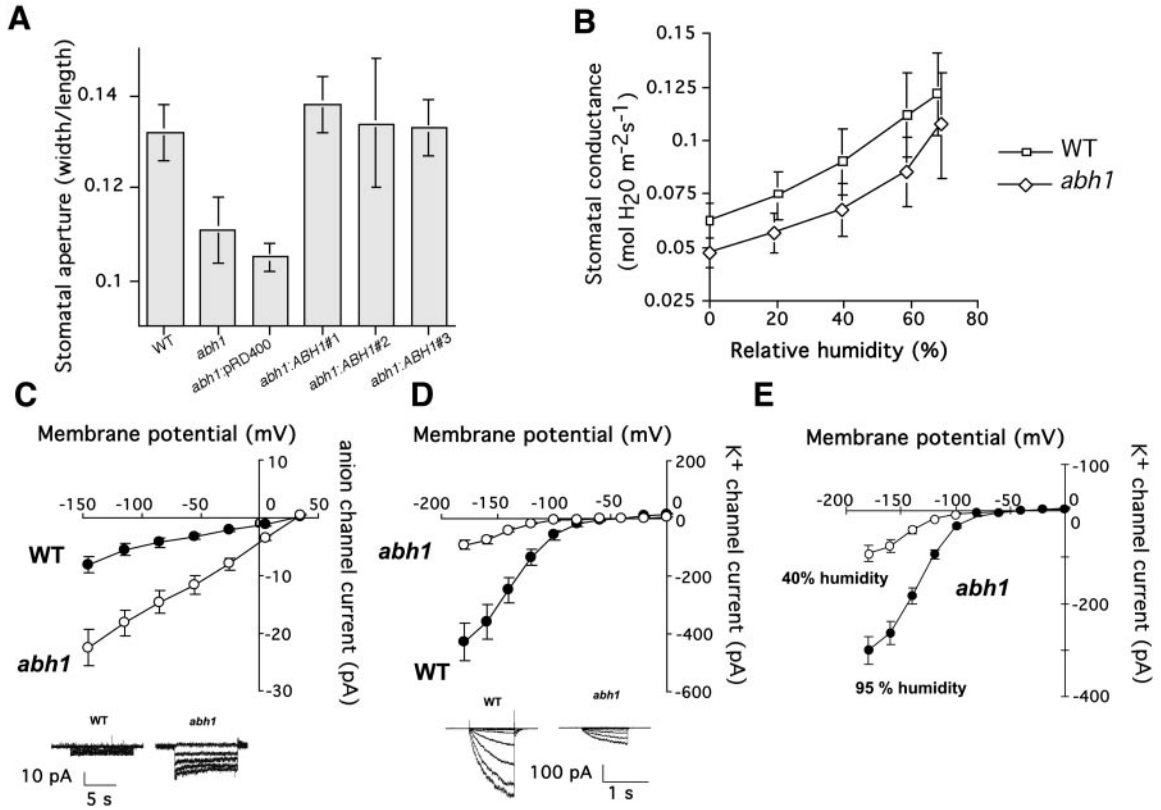

Figure 7. Stomatal aperture and guard cell anion and K^+_{in} channel activity are modified in *abh1*. A, Stomatal apertures in *abh1* are smaller than in WT in plants grown at 40% humidity. Leaves were directly harvested from plants grown in a 40% humidity growth chamber and stomatal apertures were measured without any pre-incubation in opening solution. Three independent *abh1* lines complemented with the *ABH1* locus (*abh1*:*ABH1* nos. 1, 2, and 3) show stomatal apertures similar to WT. *abh1* control plants transformed with vector only (*abh1*:pRD400) show *abh1* stomatal apertures. The data represent the mean ± SD of three independent experiments. B, Relative changes in leaf gas exchange in response to different humidity levels are similar in *abh1* and WT. Stomatal conductance of WT and *abh1* at several humidities was measured in intact leaves using a Li-6400 infrared gas analyzer (LI-COR, Inc., Lincoln, NE). Stomata were acclimated first to a high humidity (≥80% RH), then the humidity was sequentially dropped and new steady-state conductances determined at each humidity level. New steady states were achieved within 5 to 15 min after the humidity step. Data represent the mean ± SE of three independent experiments. C and D, Whole-cell current voltage relationships recorded in WT and *abh1* guard cells isolated from 40% humidity-grown plants showed a constitutive activation of slow anion channel currents and a decreased inward-rectifying K^+ (K^+_{in}) channel activity in *abh1* compared with WT (WT, $n = 26$ [C]; $n = 13$ [D]) and (*abh1*: $n = 35$ [C]; $n = 14$ [D]). Inserts show examples of ion current recordings. E, Whole-cell current voltage relationships recorded in *abh1* guard cells isolated from either 40% humidity-grown plants ($n = 14$ cells) or after 72 h of high humidity (95%) treatment ($n = 17$ cells). Anion and K^+ currents were recorded from 4- to 6-week-old plants as described in "Materials and Methods."

duced stomatal apertures in *abh1* at low humidity are because of signaling mediated by endogenous ABA.

ABA induces cytosolic Ca^{2+} increases, which in turn activate slow anion channels and inhibit K^+_{in} channels in guard cells (Schroeder and Hagiwara, 1989; McAinsh et al., 1990). The activities of guard cell slow anion channels and K^+_{in} channels were investigated in *abh1* and WT grown at 40% humidity, which causes reduced stomatal apertures in *abh1* (Fig. 7A). Patch clamp experiments performed on guard cell protoplasts from plants grown under low humidity showed that in *abh1* guard cells, anion currents were consistently larger than those in the WT guard cells (Fig. 7C; $P < 0.001$). Furthermore, anion currents ($n = 6$) showed reduction to WT magnitudes in a complemented line ($P = 0.15$; data not shown). Control experiments were performed on the ABA-hypersensitive mutant, *era1-2*. In *era1-2*, no constitutive activation of guard cell anion channels was observed in the absence of exogenous ABA ($n = 8$, data not shown), confirming previous findings (Pei et al., 1998). These data show a difference in slow anion channel regulation in the absence of exogenous ABA in *abh1* (Fig. 7C) and *era1*, indicating different functions of these two negative regulators of ABA signaling.

K^+_{in} channel currents were substantially smaller in *abh1* guard cells than in WT guard cells from plants grown at 40% humidity without addition of exogenous ABA (Fig. 7D; $P < 0.001$). K^+_{in} currents ($n = 6$)

showed recovery of WT magnitudes in a complemented line ($P = 0.74$). Furthermore, when plants were exposed to high (95%) humidity for 3 d, K^+_{in} channel current magnitudes in *abh1* guard cells were significantly larger ($n = 17$) than those in *abh1* guard cells from 40% humidity-grown plants ($n = 14$) ($P < 0.001$ at -180 mV; Fig. 7E). K^+_{in} channel currents in *abh1* guard cells grown at 95% showed recovery, but remained slightly smaller than the current magnitudes of WT grown at 40% humidity (Fig. 7, D and E). Anion channel and K^+_{in} channel activities recorded in *abh1* guard cells isolated from plants grown at 40% humidity (Fig. 7, C and D) correlated with the reduced stomatal apertures and reduced gas exchange found in *abh1* leaves (Fig. 7A).

ABA Induction of Stomatal Closure in *abh1/abi1-1* and *abh1/era1-2* Double Mutants

To further investigate genetic interactions of *abh1* with previously characterized early ABA signaling mutants, stomatal responses in homozygous *abh1/era1-2* and *abh1/abi1-1* double mutants were analyzed. In the *abh1/era1-2* double mutant, stomatal closure in response to ABA was similar to the response in *abh1* alone when plants were treated overnight at high humidity (Fig. 8A). However, stomatal apertures of plants grown at 40% humidity were similar in *abh1/era1-2* and *era1-2* and similar to WT (Fig. 8B).

The complex interaction of *abh1* and *era1-2* was also observed for non-guard cell phenotypes. For example, the increased number of petals described in *era1-2* (Ziegelhoffer et al., 2000) compared with WT was also observed in the *abh1/era1-2* double mutant (data not shown), whereas the *abh1* serrated leaf phenotype (Fig. 4A) was unchanged in *abh1/era1-2* compared with *abh1*. However, the delay in growth of *abh1/era1-2* was increased compared with both *abh1* and *era1-2*, suggesting additive affects in this response (data not shown). The ability to produce siliques and seeds was strongly reduced in *abh1/era1-2* (data not shown). All these data stress the complexity by which *abh1* and *era1-2* interact in planta, suggesting that they may target distinct processes in the ABA signaling network that have differential relative importance in different tissues and depending on conditions. Furthermore, *era1* is known to have pleiotropic phenotypes because it is the only farnesyl transferase β-subunit gene in Arabidopsis; therefore, many *era1* phenotypes would be expected not to show an interaction with *abh1*. ERA1-associated mechanisms that are considered not to be linked to ABA signaling include the Wiggum flower development phenotype and farnesylation of the AP1 transcription factor (Yalovsky et al., 2000; Ziegelhoffer et al., 2000).

Stomatal apertures in response to ABA were also investigated in the *abh1/abi1-1* double mutant. As shown in Figure 9A, 1 μM ABA did not cause significant stomatal closure in the *abh1/abi1-1* double mutant, but induced stomatal closing in the WT. At 10 μM ABA, however, stomata closed in the *abh1/abi1-1* double mutants, whereas they remained widely opened in *abi1-1*. These data showed that ABA-induced stomatal closing in the *abh1/abi1-1* double mutant is more ABA sensitive than in the *abi1-1*

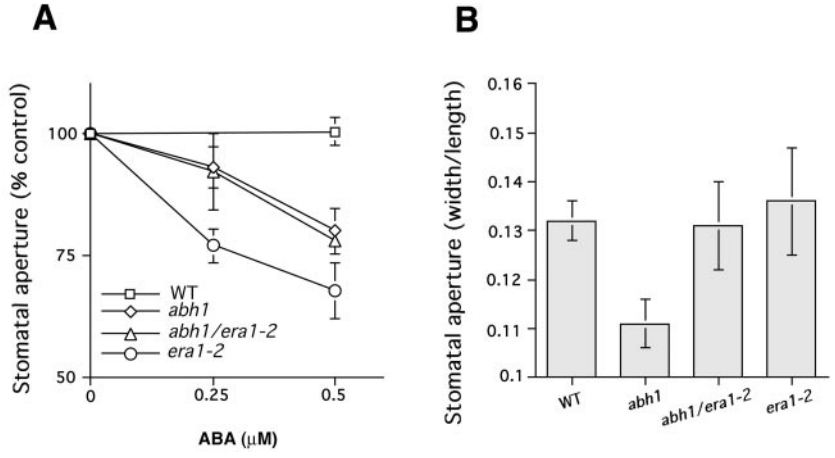

Figure 8. Stomatal aperture phenotypes in the presence and absence of ABA in the *abh1/era1-2* double mutant. A, ABA-induced stomatal closure in the *abh1/era1-2* double mutant is similar to *abh1*. Plants were kept overnight in high (95%) humidity and then leaves were pre-incubated for 2 h in opening solution, under light. ABA was then added and stomatal apertures measured after 2 more hours. Stomatal aperture is expressed relative to the mean of stomatal aperture measured with no ABA for each line. Stomatal aperture ratio (width/length) with no ABA were 0.17 ± 0.016, 0.175 ± 0.015, 0.23 ± 0.029, and 0.21 ± 0.016 for WT, *abh1*, *era1-2*, and *abh1/era1-2*, respectively. B, Stomatal apertures in *abh1/era1-2* plants grown at 40% humidity show similar opening to *era1-2* and WT. Leaves were directly harvested from plants grown in a 40% humidity growth chamber about 6 h after onset of the 16-h day/night period and stomatal apertures were measured without any pre-incubation in stomatal opening solution. Data in A and B represent the mean ± SE of three independent experiments with a minimum of 20 stomatal apertures measured per experiment and condition.

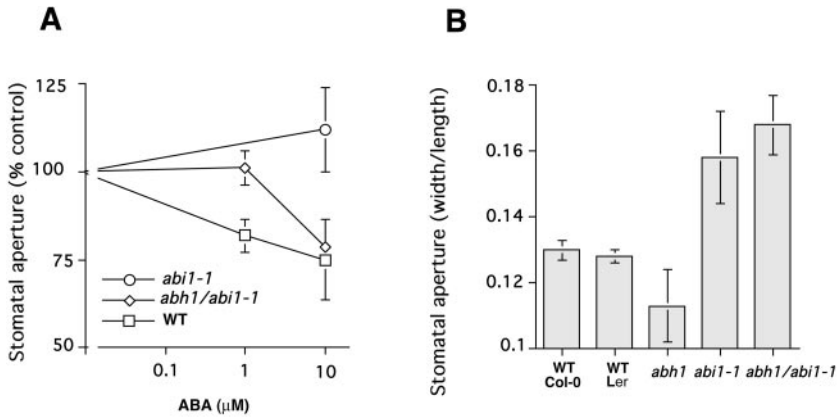

Figure 9. Stomatal aperture phenotypes in the presence or absence of ABA in the *abh1/abi1-1* double mutant. A, ABA-induced stomatal closure in *abh1/abi1-1* double mutant shows an intermediate response relative to *abi1-1* and WT. Leaves were pre-incubated for 2 h in stomatal opening solution, under light, and then ABA was added and stomatal apertures measured after 2 more h. Stomatal aperture is expressed relative to the mean of stomatal apertures measured with no ABA for each line. Stomatal aperture ratio (width/length) with no ABA were 0.187 ± 0.016, 0.194 ± 0.011, and 0.157 ± 0.015 for WT, *abh1/abi1-1*, and *abi1-1*, respectively. B, Stomatal apertures in *abh1/abi1-1* plants grown at 40% humidity are as wide as *abi1-1*. Leaves were directly harvested from plants grown in a 40% humidity growth chamber and stomatal apertures were measured without any pre-incubation in stomatal opening solution. A and B, Data represent the mean ± SD of three independent experiments.

background. These data correlate with an intermediate ABA sensitivity of the *abh1/abi1-1* double mutant in seed germination that lies between the *abh1* and *abi1-1* sensitivities (Hugouvieux et al., 2001).

However, because *abh1* and *abi1-1* mutants are in the Columbia and L*er* backgrounds, respectively, we have also isolated a control line that carries the *abi1-1* mutation in an *ERECTA* WT background, from F_2 seeds resulting from *abh1/abi1-1* crosses. The control line and its progeny showed a strong insensitivity to 10 μM ABA (stomatal aperture after ABA treatment was 93% ± 7% of the maximal stomatal aperture measured with no ABA). Transgenic expression of *abi1-1* in tobacco (*Nicotiana benthamiano*) confers strong insensitivity to ABA (Armstrong et al., 1995), confirming that the dominant *abi1-1* mutant protein functions in many backgrounds. The *abh1* mutation partially suppresses this dominant *abi1-1* phenotype.

Stomatal apertures of *abi1-1* plants, measured directly from plants grown at 40% humidity, were generally larger than those of WT plants (L*er* background; Fig. 9B). Under the same conditions, stomatal apertures in the *abh1/abi1-1* double mutant were similar to *abi1-1* (Fig. 9B). These findings are also consistent with the hypothesis that reduced stomatal apertures in *abh1* at low humidity are because of a response to low levels of endogenous ABA as the *abi1-1* mutation causes ABA insensitivity to low ABA concentrations in the *abi1-1/abh1* double mutant (Fig. 9A).

ABA-Hypersensitive Stomatal Closure in *sad1*

Mutations in three RNA-binding proteins have been described recently that show ABA hypersensitivity (Lu and Fedoroff, 2000; Hugouvieux et al., 2001; Xiong et al., 2001a). In addition to the mRNA cap binding protein ABH1 (Hugouvieux et al., 2001), these genes include a double-stranded RNA-binding protein, HYL1 (Lu and Fedoroff, 2000) and a protein with similarity to an Sm-like snRNP protein, SAD1 (Xiong et al., 2001a). We investigated whether the *sad1* and *hyl1* mutations affect stomatal movements. ABA-induced stomatal closure in the *sad1* mutant showed a reproducible ABA hypersensitivity compared with the WT ecotype C24 (Fig. 10). In contrast, in the *hyl1* mutant, ABA-induced stomatal closure was similar to the WT ecotype Nossen in two independent lines of investigation (N. Fedoroff, personal communication; $n = 3$ independent experiments; data not shown).

DISCUSSION

In a previous report, we described the isolation and characterization of a new recessive ABA-hypersensitive Arabidopsis mutant, *abh1*. *abh1* shows ABA hypersensitivity in seed germination, stomatal closure, and ABA-induced guard cell calcium increases (Hugouvieux et al., 2001). ABH1 was shown to function in vitro as a subunit of a dimeric mRNA CBC and *ABH1* gene expression is necessary for the correct expression level of a subset of genes in the Arabidopsis genome (Hugouvieux et al., 2001). The isolation of *abh1* points to a link between mRNA metabolism and correct ABA signaling.

To better understand ABH1 function at the whole-plant level and in guard cells, we further investigated *ABH1* gene expression and regulation, ABH1 protein localization, and we further characterized *abh1* mutant phenotypes, *sad1* and *hyl1* phenotypes in guard

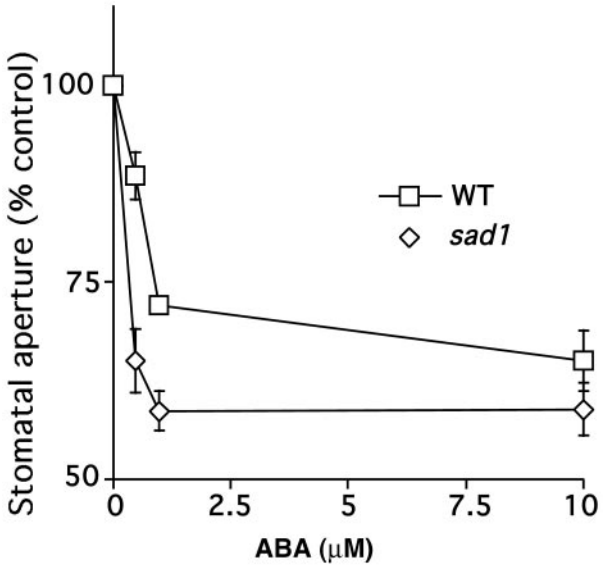

Figure 10. ABA-hypersensitive stomatal closing in the *sad1* mutant. Plants were kept overnight in high (95%) humidity and then leaves were pre-incubated for 2 h in opening solution, under light. ABA was then added and stomatal apertures measured after 2 more h in *sad1* and WT C24 ecotype. Stomatal apertures are expressed relative to the mean stomatal apertures measured without ABA addition for each line. Stomatal aperture ratios (width/length) without ABA addition were 0.158 ± 0.01 and 0.145 ± 0.006 for WT and *sad1*, respectively. Data represent the mean ± SE of three independent experiments. Error bars are smaller than symbols when not visible.

cells, and genetic interactions between *ABH1* and two well-described early ABA signaling components, *ERA1* and *abi1-1*.

ABH1 Expression Pattern and Nuclear Localization

The *ABH1* gene is expressed in all tissues tested (Figs. 1 and 2). However, our data further show that the *ABH1* expression level varies between tissues and also appears to depend on the developmental stage. Further research will be needed to determine whether different expression levels affect ABH1 functions in these tissues or at these developmental stages. It is intriguing to note that the *abh1* mutation has no visible impact on flower morphology even though *ABH1* mRNA levels are high (Fig. 1). Thus, it is possible that some ABH1 functions may be conditional and/or that this expression pattern is related to the *abh1* phenotype in seeds.

ABH1 expression does not appear to be affected by external ABA application (Fig. 3), nor by drought stress. Similar results were observed in the case of the *SAD1* gene (Xiong et al., 2001a). In humans, CBC activity is increased in response to growth factors (Wilson et al., 1999). It has been proposed that this increased CBC activity may be because of posttranslational modification of the ABH1 homolog, CBP80; for example, by phosphorylation (Wilson and Cerione, 2000), although direct evidence has not been yet reported. The CBC is also known to interact with several proteins from the spliceosome complex and translation machinery (Fortes et al., 2000; Ishigaki et al., 2001; McKendrick et al., 2001). The x-ray crystal structure of a human CBC was recently determined and suggested that CBP80 could behave as a platform protein for nuclear cap-related RNA-processing proteins (Mazza et al., 2001). Thus, it is tempting to speculate that in response to ABA, ABH1 activity may be regulated by posttranslational modifications and/or interaction with new regulators. Note that *sad1* does not interact in yeast two-hybrid experiments with either ABH1 or AtCBP20 (Xiong et al., 2001a). However, a larger complex that includes these proteins cannot be excluded.

Using protein database motif searches, no clear nuclear localization signal can be detected in the ABH1 protein sequence, in contrast to the human and yeast homologs (data not shown). The *abh1* mutant was complemented by an N-terminal GFP-ABH1 fusion protein, which was predominantly localized to the nucleus (Fig. 6). In contrast, a C-terminal ABH1-GFP fusion did not complement *abh1*. The ABH1 protein has a C-terminal extension compared with yeast and animal CBP80 that could be related to specific unknown properties of ABH1 (Hugouvieux et al., 2001).

The nuclear localization correlates with the function of ABH1 as a subunit of a nuclear CBC as described in yeast and mammals (Lewis and Izaurralde, 1997). We also observed a slight GFP fluorescence in the cytosol (Fig. 6). Although the steady-state level of CBC is mainly nuclear, it is well established that CBC moves into the cytosol during mRNA export in yeast, insects, and vertebrates and is later recycled back into the nucleus (Goerlich et al., 1996; Visa et al., 1996; Shent et al., 2000).

Whole-Plant and Stomatal Responses of *abh1*

Although *ABH1* is expressed in several plant tissues, *abh1* plants showed only a slightly slowed growth, a serrated leaf phenotype, and a slightly smaller stem length at maturity compared with WT (Figs. 4 and 5; Table I). No other clearly visible phenotypes were detected at the morphological level. Similarly, the yeast mutant disrupted in *CBP80* shows a growth delay compared with WT, depending on the carbon source used (Uemura and Jigami, 1992).

In the present study, we characterized further *abh1* phenotypes in guard cells. *abh1* stomatal pore apertures were significantly reduced compared with WT when plants were grown in a growth chamber at 40% humidity (Fig. 7A). Reduced stomatal apertures correlated with both a constitutive activation of slow anion channels and a reduction in K^+_{in} channel activity in *abh1* guard cells (Fig. 7, B, C, and E). The stomatal phenotype of *abh1* plants grown at 40%

humidity correlates with ion channel activities, even though ion channel activities were measured after protoplastation (see "Materials and Methods"). These data suggest that the modulation of ion channel activities in *abh1* revealed here may be because of longer term regulatory mechanisms such as posttranslational modification and/or potential alteration of expression levels of ABA transducers (Hugouvieux et al., 2001).

Slow anion channels are activated by cytosolic Ca^{2+} elevations and ABA (Schroeder and Hagiwara, 1989; Grabov et al., 1997; Pei et al., 1997; Allen et al., 1999) and K^+_{in} channels are down-regulated by cytosolic Ca^{2+} elevations and by ABA (Schroeder and Hagiwara, 1989; Blatt and Armstrong, 1993). ABA content in *abh1* and WT plants are similar in sufficiently watered plants, and ABA content increased to the same extent in both WT and *abh1* after desiccation (Hugouvieux et al., 2001). The primary responses of *abh1* and WT stomates to rapid humidity changes were similar (Fig. 7B). Therefore, we propose that reduced stomatal apertures observed in *abh1* at 40% humidity are because of a response to endogenous ABA. This model is supported by the finding that *abh1/abi1-1* double mutants do not show reduced stomatal apertures at 40% humidity (Fig. 9B) and that *abi1-1* does not function in humidity signaling (Assmann et al., 2000).

The *abh1/era1-2* double mutant shows an additive ABA-hypersensitive phenotype in seed germination assays (Hugouvieux et al., 2001). Interestingly, ABA-induced stomatal closure in the *abh1/era1-2* double mutant does not show additive effects of the two mutants (Fig. 8). Under the imposed conditions, the *abh1/era1-2* double mutant showed an ABA hypersensitivity similar to *abh1*. However, when stomatal apertures were measured in plants grown at 40% humidity, stomatal apertures of the double mutant were similar to those in *era1-2* stomatal apertures (Fig. 8B). These data suggest complex interactions of the *abh1* and *era1-2* mutants, indicating that they affect different components or branches in ABA signaling that change their relative contribution to ABA signal transduction depending on conditions. In the *abh1/abi1-1* double mutant, however, ABA sensitivity was decreased compared with the *abi1-1* mutant (Fig. 9B), which correlated with seed germination assays in response to ABA (Hugouvieux et al., 2001), suggesting a less complex interaction of *abi1-1* and ABH1, which may be explained by the dominant nature of the *abi1-1* mutant.

Distinct ABA Responses in Guard Cells of *sad1* and *abh1* Compared with *hyl1*

The Sm-like snRNP protein, SAD1, was suggested to function in mRNA processing in ABA signaling and homeostasis (Xiong et al., 2001a). The independent isolation of *abh1* and *sad1* by two different screens strengthens the recent hypothesis that mRNA-processing proteins function as negative regulators in ABA signaling. Furthermore, the recessive double-stranded RNA-binding protein mutant *hyl1* also shows ABA hypersensitivity (Lu and Fedoroff, 2000). In the present study, we analyzed stomatal responses of *sad1* and *hyl1*. Although *sad1* showed ABA hypersensitivity in stomatal movement responses (Fig. 10), *hyl1* did not (data not shown; N. Fedoroff, personal communication). These data suggest that *hyl1* may modulate ABA signaling via a mechanism independent of *abh1* and *sad1*. These results are consistent with the finding that HYL1 binds double-stranded RNA, which appears to be mechanistically different from the proposed SAD1 function and ABH1 cap-binding activity. Furthermore, the *hyl1* mutation also modulates the sensitivity to auxin and cytokinin (Lu and Fedoroff, 2000), showing a clear difference from *abh1* and *sad1* (Hugouvieux et al., 2001; Xiong et al., 2001a).

Although both *sad1* and *abh1* show hypersensitivity to exogenous ABA (Fig. 10; Hugouvieux et al., 2001), there are distinct differences in the two mutants. The *sad1* mutation results in reduced ABA levels in drought-stressed plants because of a feedback mechanism from ABA signaling to ABA biosynthesis (Xiong et al., 2001a). Consistent with these findings, detached *sad1* rosettes showed an enhanced transpiration rate compared with WT (Xiong et al., 2001a). In contrast, the *abh1* mutation does not affect endogenous ABA levels and *abh1* causes reduced transpiration (Hugouvieux et al., 2001) and reduced stomatal apertures. Despite these differences, it is conceivable that ABH1 and SAD1 participate in a complex RNA-processing network that modulates ABA signaling, in such a manner that the two mutants have clearly distinguishable effects but some similarities in their phenotypes, which include ABA hypersensitivity in seed germination (Hugouvieux et al., 2001; Xiong et al., 2001) and in stomatal closing (Fig. 10).

CONCLUSIONS

In conclusion, we show that *ABH1* is widely expressed in plants and that ABH1 shows preferentially nuclear localization. The negative regulators of ABA signaling, ABH1 and the farnesyl transferase β-subunit ERA1, show complex genetic interactions and differential effects indicating that these two genes act at different locations in the ABA signal network. Findings that both *abh1* and *sad1* show similar sensitivity to exogenous ABA, whereas the *hyl1* mutant did not affect stomatal apertures in response to ABA, further strengthen the hypothesis that RNA processing modulates early ABA signaling.

MATERIALS AND METHODS

Plant Growth and Culture Conditions

abh1, other Arabidopsis mutants, and the corresponding WT ecotypes were grown side by side in growth chambers: 40% humidity, 16-h-light/8-

h-dark cycle, temperature 20°C, and photon fluency rate of 75 μmol m^{-2} s^{-1}. Unless otherwise stated, WT plants are from the Columbia ecotype. When required, the growth of *abh1* and WT plants was synchronized by sowing *abh1* plants 1 week earlier than WT. To test the sensitivity of seeds to ABA, in the case of *abh1* lines complemented with the N-terminal GFP-ABH1 fusion, seeds were plated on minimal medium (0.25× Murashige and Skoog medium) containing 0.3 μM ABA. After 4 d at 4°C, seeds were transferred to 28°C and continuous light and germination was scored after 5 more d. Seeds used for comparative studies were from plants grown and harvested in parallel. For seedling growth assays, 6-month-old *abh1* and WT seeds were germinated on Murashige and Skoog plates. Germination was scored after 2 d to make sure that all the seedlings were at the two-cotyledon stages and the root length was estimated using a micrometer under a dissecting microscope. Seeds that showed a delay in germination were removed from the plates in both WT and *abh1*. After 2, 6, 9, and 11 d of growth, root length was measured and the development of the shoot was studied by analyzing the appearance and development of new leaves under the microscope.

GFP-ABH1 Fusion Constructs and Plant Transformation

To generate N- and C-terminal fusion proteins between ABH1 and GFP proteins, the full-length *ABH1* cDNA was amplified using *Pfu* DNA polymerase (Stratagene, La Jolla, CA). Primers used for PCR included specific restriction sites at both ends, to allow the cloning of *ABH1* and *GFP* in frame in the vector GFP-JFH1 (kindly provided by Dr. Jeff Harper, The Scripps Research Institute, La Jolla, CA). PCR-amplified constructs were confirmed by sequencing (Retrogen, San Diego). *Agrobacterium tumefaciens* strain C58 was used to generate transgenic Arabidopsis plants using the floral dip technique (Clough and Bent, 1998).

Confocal Microscopy

The subcellular localization of ABH1 fused to GFP was assessed by scanning confocal laser microscopy in epidermal strips prepared as described (Allen et al., 1999). Epidermal strips were mounted between two cover slips on an Axiovert 35M microscope (Zeiss, Jena, Germany) coupled to an MCr-1000 scanning laser confocal system (Bio-Rad Laboratories, Hercules, CA). Argon laser light (488-nm wavelength, 30% power) was used to excite GFP and emission light was measured at 522 nm. Transmission images were collected in parallel. Autofluorescence was monitored at 488 nm.

GUS Staining

GUS activity was assayed on either seedlings grown on Murashige and Skoog plates or soil, after 24 h of incubation in a solution containing 2 mM 5-bromo-4-chloro-3-indolyl-β-D-glucuronide, 0.1 M Na_2HPO_4 (pH 7.2), 0.1% (w/v) K^+ ferrocyanide, 0.1% (w/v) ferricyanide, and 0.1% (v/v) Triton. Experiments were performed on three independent WT:ABH1-GUS lines. WT control plants showed no GUS activity (data not shown).

RNA-Blot Analyses

Total RNA was extracted from flowers, leaves, stems, and roots of 5- to 6-week-old WT plants using Trizol reagent (Life Technologies/Gibco-BRL, Rockville, MD). Poly(A^+) RNA was further purified using the μMACS mRNA Isolation Kit (Miltenyi Biotec, Auburn, CA) according to the manufacturer's instructions. To examine whether ABA regulates *ABH1* gene expression, total RNA and poly(A^+) RNA were extracted from rosette leaves of WT plants sprayed with 100 μM ABA, 4 h before extraction. Several complementary experiments were carried out using 1, 10, and 100 μM ABA for different application times. Total and poly(A^+) RNA were separated in a 1.2% (w/v) denaturing agarose gel, and then transferred onto a Hybond N^+ membrane (Amersham, Buckinghamshire, UK). The blots were hybridized with ^{32}P-labeled *ABH1* cDNA and/or a *Cor47* genomic fragment amplified by PCR using the forward and reverse primers, 5'GAT CGA AAT GGT TGA TAA GAG ATC3' and 5'CAC ACT CTC CGA CAC TGG TAC C3', respectively.

Stomatal Movement Analyses

Stomatal aperture measurements were performed as described (Pei et al., 1997; Allen et al., 2000). Stomata from 5- to 6-week-old plants were opened by exposing excised leaves for 2 h to white light (intensity: 125 μmol m^{-2} s^{-1}), floating in a stomatal opening solution containing 5 mM KCl, 10 μM $CaCl_2$, and 10 mM MES (pH 6.15), in the growth chamber at 20°C. Stomatal apertures were measured 2 h after ABA was added (Pei et al., 1997). When experiments were performed with *abh1*, *era1-2*, *sad1*, and *abh1/era1-2* double mutants, plants were subjected to an overnight high (95%) humidity treatment before incubation of the leaves in stomatal opening solution. Control experiments were performed in parallel with no ABA added. Leaves were then blended for 30 s and epidermal peels collected as described (Allen et al., 1999). Stomatal apertures were measured (pore width/length) by focusing on the focal plane of guard cells in epidermal strips (Ichida et al., 1997).

Stomatal Conductance

Stomatal responses to humidity were determined by measuring transpiration rates using a Li-6400 infrared gas analyzer (LI-COR, Inc.). Chamber temperature and carbon dioxide concentration were maintained at 23°C and 400 μL L^{-1}, respectively. Constant illumination of 500 μmol quanta $m^{-2}s^{-1}$ photosynthetically active radiation was provided by a red and blue LED light source.

Electrophysiology

Anion and K^+ currents were recorded from guard cell protoplasts of 4- to 6-week-old plants (Ichida et al., 1997; Pei et al., 1997) grown either at 40% humidity or after 72 h of high-humidity treatment (95%). The solutions used in patch clamp experiments were composed of 150 mM CsCl, 2 mM $MgCl_2$, 6.7 mM EGTA, 3.35 mM $CaCl_2$, and 10 mM HEPES-Tris, pH 7.1, in the pipette medium and of 30 mM CsCl, 2 mM $MgCl_2$, 1 mM $CaCl_2$, and 10 mM MES-Tris, pH 5.6, in the bath medium, for anion channel activity measurement (Pei et al., 1997). For K^+ current measurements, the pipette solution was composed of 30 mM KCl, 70 mM-Glu, 2 mM $MgCl_2$, 6.7 mM EGTA, 3.35 mM $CaCl_2$, 5 mM ATP, and 10 mM HEPES-Tris, pH 7.1. The bath solution contained 30 mM KCl, 40 mM $CaCl_2$, 2 mM $MgCl_2$, and 10 mM MES-Tris, pH 5.5 (Pei et al., 1997). For all solutions, osmolarity was adjusted to 485 mmol kg^{-1} for bath solutions and 500 mmol kg^{-1} for pipette solutions by addition of D-sorbitol.

ACKNOWLEDGMENTS

We thank Gethyn Allen for advice on confocal microscopy and members of the laboratory for discussions, and David Waner, Christine Salomon, and Jorieth Jose for assistance. We thank Drs. Nina Fedoroff and Jian-Kang Zhu for providing *hyl1* and *sad1* mutants and for discussion.

Received June 4, 2002; returned for revision July 8, 2002; accepted August 12, 2002.

LITERATURE CITED

Allen GJ, Chu SP, Schumacher K, Shimazaki CT, Vafeados D, Kemper A, Hawke SD, Tallman G, Tsien RY, Harper JF et al. (2000) Alteration of stimulus-specific guard cell calcium oscillations and stomatal closing in *Arabidopsis det3* mutant. Science **289:** 2338–2342

Allen GJ, Kuchitsu K, Chu SP, Murata Y, Schroeder JI (1999) *Arabidopsis abi1-1* and *abi2-1* phosphatase mutations reduce abscisic acid-induced cytoplasmic calcium rises in guard cells. Plant Cell **11:** 1785–1798

Armstrong F, Leung J, Grabov A, Brearley J, Giraudat J, Blatt MR (1995) Sensitivity to abscisic acid of guard-cell K^+ channels is suppressed by *abi1-1*, a mutant *Arabidopsis* gene encoding a putative protein phosphatase. Proc Natl Acad Sci USA **92:** 9520–9524

Assmann SM, Snyder JA, Lee Y-RJ (2000) ABA-deficient (*aba1*) and ABA-insensitive (*abi1-1*, *abi2-1*) mutants of *Arabidopsis* have a wild-type stomatal response to humidity. Plant Cell Environ **23:** 387–395

Blatt MR, Armstrong F (1993) Potassium channels of stomatal guard cells: abscisic acid-evoked control of the outward rectifier mediated by cytoplasmic pH. Planta **191:** 330–341

Clough SJ, Bent AF (1998) Floral dip: a simplified method for *Agrobacterium*-mediated transformation of *Arabidopsis thaliana*. Plant J **16:** 735–743

Cutler S, Ghassemian M, Bonetta D, Cooney S, McCourt P (1996) A protein farnesyl transferase involved in abscisic acid signal transduction in *Arabidopsis*. Science **273:** 1239–1241

Finkelstein RR, Gampala SS, Rock CD (2002) Abscisic acid signaling in seeds and seedlings. Plant Cell Suppl **14:** S15–45

Finkelstein RR, Lynch TJ (2000) The *Arabidopsis* abscisic acid response gene *ABI5* encodes a basic leucine zipper transcription factor. Plant Cell **12:** 599–609

Finkelstein RR, Wang ML, Lynch TJ, Rao S, Goodman HM (1998) The *Arabidopsis* abscisic acid response locus *ABI4* encodes an APETALA 2 domain protein. Plant Cell **10:** 1043–1054

Fortes P, Inada T, Preiss T, Hentze MW, Mattaj IW, Sachs AB (2000) The yeast nuclear cap binding complex can interact with translation factor elF4G and mediate translation initiation. Mol Cell **6:** 191–196

Giraudat J, Hauge BM, Valon C, Smalle J, Parcy F, Goodman HM (1992) Isolation of the *Arabidopsis ABI3* gene by positional cloning. Plant Cell **4:** 1251–1261

Görlich D, Kraft R, Kostka S, Vogel F, Hartmann E, Laskey RA, Mattaj IW, Izaurralde E (1996) Importin provides a link between nuclear protein import and UsnRNA export. Cell **87:** 21–32

Grabov A, Leung J, Giraudat J, Blatt MR (1997) Alteration of anion channel kinetics in wild-type and *abi1-1* transgenic *Nicotiana benthamiana* guard cells by abscisic acid. Plant J **12:** 203–213

Hugouvieux V, Kwak JM, Schroeder JI (2001) An mRNA cap binding protein, ABH1, modulates early abscisic acid signal transduction in *Arabidopsis*. Cell **106:** 477–487

Ichida AM, Pei Z-M, Baizabal-Aguirre VM, Turner KJ, Schroeder JI (1997) Expression of a Cs^+-resistant guard cell K^+ channel confers CS^+-resistant, light-induced stomatal opening in transgenic Arabidopsis. Plant Cell **9:** 1843–1857

Ishigaki Y, Li X, Serin G, Maquat LE (2001) Evidence for a pioneer round of mRNA translation: mRNAs subject to nonsense-mediated decay in mammalian cells are bound by CBP80 and CBP20. Cell **106:** 607–617

Koornneef M, Leon-Kloosterziel KM, Schwartz SH, Zeevaart JAD (1998) The genetic and molecular dissection of abscisic acid biosynthesis and signal transduction in *Arabidopsis*. Plant Physiol Biochem **36:** 83–89

Lemichez E, Wu Y, Sanchez JP, Mettouchi A, Mathur J, Chua NH (2001) Inactivation of AtRac1 by abscisic acid is essential for stomatal closure. Genes Dev **15:** 1808–1816

Leung J, Bouvier-Durand M, Morris PC, Guerrier D, Chefdor F, Giraudat J (1994) *Arabidopsis* ABA response gene *ABI1*: features of a calcium-modulated protein phosphatase. Science **264:** 1448–1452

Leung J, Giraudat J (1998) Abscisic acid signal transduction. Annu Rev Plant Physiol Plant Mol Biol **49:** 199–222

Leung J, Merlot S, Giraudat J (1997) The *Arabidopsis* abscisic acid-insensitive2 (*ABI2*) and *ABI1* genes encode homologous protein phosphatases 2C involved in abscisic acid signal transduction. Plant Cell **9:** 759–771

Lewis JD, Izaurralde E (1997) The role of the cap structure in RNA processing and nuclear export. Euro J Biochem **247:** 461–469

Li J, Wang X-Q, Watson MB, Assmann SM (2000) Regulation of abscisic acid-induced stomatal closure and anion channels by guard cell AAPK kinase. Science **287:** 300–303

Lu C, Fedoroff N (2000) A mutation in the *Arabidopsis HYL1* gene encoding a dsRNA binding protein affects responses to abscisic acid, auxin, and cytokinin. Plant Cell **12:** 2351–2366

MacRobbie EAC (1998) Signal transduction and ion channels in guard cells. Philos Trans R Soc London **353:** 1475–1488

Marcotte WR, Guiltinan MJ, Quatrano RS (1992) ABA-regulated gene expression: *cis*-acting sequences and trans-acting factors. Biochem Soc Trans **20:** 93–97

Mazza C, Ohno M, Segref A, Mattaj IW, Cusack S (2001) Crystal structure of the human nuclear cap binding complex. Mol Cell **8:** 383–396

McAinsh MR, Brownlee C, Hetherington AM (1990) Abscisic acid-induced elevation of guard cell cytosolic calcium precedes stomatal closure. Nature **343:** 186–188

McKendrick L, Thompson E, Ferreira J, Morley SJ, Lewis JD (2001) Interaction of eukaryotic translation initiation factor 4G with the nuclear cap-binding complex provides a link between nuclear and cytoplasmic functions of the m^7 guanosine cap. Mol Cell Biol **21:** 3632–3641

Meyer K, Leube MP, Grill E (1994) A protein phosphatase 2C involved in ABA signal transduction in *Arabidopsis thaliana*. Science **264:** 1452–1455

Pei Z-M, Ghassemian M, Kwak CM, McCourt P, Schroeder JI (1998) Role of farnesyltransferase in ABA regulation of guard cell anion channels and plant water loss. Science **282:** 287–290

Pei Z-M, Kuchitsu K, Ward JM, Schwarz M, Schroeder JI (1997) Differential abscisic acid regulation of guard cell slow anion channels in *Arabidopsis* wild-type and *abi1* and *abi2* mutants. Plant Cell **9:** 409–423

Schroeder JI, Allen GJ, Hugouvieux V, Kwak JM, Waner D (2001) Guard cell signal transduction. Annu Rev Plant Physiol Plant Mol Biol **52:** 627–658

Schroeder JI, Hagiwara S (1989) Cytosolic calcium regulates ion channels in the plasma membrane of *Vicia faba* guard cells. Nature **338:** 427–430

Shent EC, Stage-Zimmermann T, Chui P, Silver PA (2000) The yeast mRNA-binding protein Npl3p interacts with the cap-binding complex. J Biol Chem **275:** 23718–23724

Uemura H, Jigami Y (1992) GCR3 encodes an acidic protein that is required for expression of glycolytic genes in *Saccharomyces cerevisiae*. J Bacteriol **174:** 5526–5532

Visa N, Izaurralde E, Ferreira J, Daneholt B, Mattaj IW (1996) A nuclear cap-binding complex binds Balbiani ring pre-mRNA cotranscriptionally and accompanies the ribonucleoprotein particle during nuclear export. J Cell Biol **133:** 5–14

Wang XQ, Ullah H, Jones AM, Assmann SM (2001) G protein regulation of ion channels and abscisic acid signaling in *Arabidopsis* guard cells. Science **292:** 2070–2072

Wilson KF, Cerione RA (2000) Signal transduction and post-transcriptional gene expression. Biol Chem **381:** 357–365

Wilson KF, Fortes P, Singh US, Ohno M, Mattaj IW, Cerione RA (1999) The nuclear cap-binding complex is a novel target of growth factor receptor-coupled signal transduction. J Biol Chem **274:** 4166–4173

Xiong L, Gong Z, Rock CD, Subramanian S, Guo Y, Xu W, Galbraith D, Zhu JK (2001a) Modulation of abscisic acid signal transduction and biosynthesis by an Sm-like protein in Arabidopsis. Dev Cell **1:** 771–781

Xiong L, Lee B-h, Ishitani M, Lee H, Zhang C, Zhu J-K (2001b) *FIERY1* encoding an inositol polyphosphate 1-phosphatase is a negative regulator of abscisic acid and stress signaling in *Arabidopsis*. Genes Dev **15:** 1971–1984

Yalovsky S, Rodriguez-Concepcion M, Bracha K, Toledo-Ortiz G, Gruissem W (2000) Prenylation of the floral transcription factor APETALA1 modulates its function. Plant Cell **12:** 1257–1266

Ziegelhoffer EC, Medrano LJ, Meyerowitz EM (2000) Cloning of the *Arabidopsis* WIGGUM gene identifies a role for farnesylation in meristem development. Proc Natl Acad Sci USA **97:** 7633–7638

